PHYSICAL REVIEW D **85,** 083008 (2012)

Origin of TeV Galactic cosmic rays

A. Neronov[1,*] and D. V. Semikoz[2,3,†]

[1]*ISDC Data Centre for Astrophysics, Ch. d'Ecogia 16, 1290, Versoix, Switzerland*
[2]*APC, 10 rue Alice Domon et Leonie Duquet, F-75205 Paris Cedex 13, France*
[3]*Institute for Nuclear Research RAS, 60th October Anniversary prospect 7a, Moscow, 117312, Russia*

(Received 23 January 2012; published 25 April 2012)

We consider a possibility of identification of sources of cosmic rays (CR) of the energy above 1 TeV via observation of degree-scale extended γ-ray emission which traces the locations of recent sources in the Galaxy. Such emission in the energy band above 100 GeV is produced by CR nuclei and electrons released by the sources and spreading into the interstellar medium. We use the data from the Fermi γ-ray telescope to locate the degree-scale 100 GeV γ-ray sources. We find that the number of such sources and their overall power match to those expected when CRs injection events happen every $\sim$100 yr in portions of $\sim 10^{50}$ erg. We find that most of the sources are associated to pulsars with spin-down age less than $\sim$30 kyr and hence to the recent supernova explosions. This supports the hypothesis of supernova origin of Galactic CRs. We notice that the degree-scale extended emission does not surround shell-like supernova remnants without pulsars. Based on this observation, we argue that the presence of the pulsar is essential for the CR acceleration process. We expect that a significant fraction of the degree-scale sources should be detectable as extended sources with km^3-scale neutrino detectors.

DOI: 10.1103/PhysRevD.85.083008 PACS numbers: 98.70.Sa, 95.85.Pw

I. INTRODUCTION

The bulk of the cosmic ray (CR) flux hitting the Earth's atmosphere is composed of protons and heavy nuclei with energies in the 1–10 GeV range [1,2]. They are injected into the interstellar medium (ISM) by unknown sources and spread across the ISM via diffusion in the turbulent interstellar magnetic field. The diffusive propagation of CRs provides a major obstacle for identification of the CR sources: angular distribution and spectral properties of CRs captured by particle detectors mostly provide information on the details of the process of diffusion of CRs through the Galactic magnetic field rather than on the location of the CR sources and mechanisms of particle acceleration in the sources.

Information on the details of diffusion of the CRs through the ISM, obtained from the particle detector measurements, provides a constraint on the energy output of the Galactic CR sources. The CR data suggest that typical CR particles spend only $t_{\rm CR} \leq 10^7$ yr in the Galactic disk before escaping to the larger halo and/or to the intergalactic medium [1–4]. Constraint on the lifetime of CRs in the Galaxy imposes a constraint on the cumulative time-average power of the CR sources, $L_{\rm CR} \sim 10^{41}$ erg/s [1–4], needed to support the observed CR energy density $\simeq 1$ eV/cm^3 [5].

This power could be supplied e.g. by supernovae if some $\sim$0.1% of the energy output of the gravitational collapse of the star is transferred to the CRs [1,6]. Several types of the supernova-related phenomena are known to be associated to particle acceleration: γ-ray bursts (GRBs), pulsars and the associated pulsar wind nebulae (PWN), and supernova remnant (SNR) shells. Particle acceleration to the energies $\gtrsim$ 1–10 GeV is now firmly established from the γ-ray band observations of all the three types of objects [7,8].

Alternatively, the required power could be provided by acceleration process which operates at the distance and time scales larger than individual supernova remnants e.g. in superbubbles [9–11] and/or even continuously throughout the Galaxy (see Ref. [12] and references therein). Evidence in favor of such scenario is found from the study of chemical composition of the low-energy cosmic ray flux [13–15] and from the direct association of GeV band extended emission with particle acceleration in Cygnus superbubble [11].

Clarification of the physical mechanism responsible for the CR production requires localization of the CR sources in space. This could, in principle, be done using γ-ray observations. This possibility arises because CRs confined in the source could interact with low-energy particles producing γ-rays and neutrinos. However, identification of the CR sources among the Galactic γ-ray sources suffers from large uncertainties. In most of the cases it is not clear if the amount of target material in the source is sufficiently large for the production of detectable CR interaction related γ-ray emission. Moreover, in most of the sources protons and nuclei are accelerated together with electrons. The accelerated electrons produce γ-ray emission via inverse Compton and Bremsstrahlung mechanisms, with intensity larger than that of the γ-ray emission from CR interactions. As a result, the ''hadronic'' component of the γ-ray flux is hidden behind much stronger ''leptonic'' γ-ray emission [16]. If CRs are injected by a process

*andrii.neronov@unige.ch
†dmitri.semikoz@apc.univ-paris7.fr

operating on large distance scales in the Galaxy, γ-ray observations might not reveal individual isolated CR sources at all [12].

Taking into account these difficulties, we consider in this paper an alternative method for the identification of the Galactic CR sources based on the γ-ray data. Instead of searching for the γ-ray emission from CR interactions in the sources, we consider the γ-ray emission produced by CRs which escape from the source and start to spread into the ISM. CRs penetrating into the ISM interact with the ISM particles and produce γ-rays via the same mechanism as inside the sources, but on much larger distance and time scales. The overabundance of CRs around the individual sources leads to the increased CR-ISM interaction rate from an extended region around the source [16]. This results in the appearance of extended γ-ray emission. We show that such extended emission around CR sources becomes detectable in the very-high-energy (VHE) band above $\sim$100 GeV. We identify the extended Galactic sources of $\gtrsim 100$ GeV γ-rays in the data of the Large Area Telescope (LAT) on board of Fermi satellite [17]. We study the overall distribution and energetics of the degree-scale sources in the Galaxy. The source statistics and morphology are consistent with the assumption that the extended γ-ray emission is produced by the CR interactions. We show that extended VHE γ-ray emission is found around all known nearby pulsar-producing supernova events which occurred in the last 30 kyr, as expected if the Galactic CRs are injected by the supernovae. We further argue that the presence of the young pulsars inside most of the degree-scale extended sources points to the possibility that CRs *with energies above* 1 TeV are injected by the PWN or by the composite SNR (shell-like SNR confining a PWN) systems, while distributed acceleration of cosmic rays in shocks produced by multiple supernovae and stellar wind bubbles might be most important at lower energies.

II. LOCATING THE CR SOURCES

CRs which escape from sources can be traced as they spread into the ISM. They could be detected via the γ-ray emission produced in CR interactions with the ISM particles. CRs of the energy $E_{\rm CR}$ diffuse through the Galactic magnetic field. Measurements of the energy-dependent diffusion coefficient based on the local measurements of the primary and secondary CR nuclei and on the modeling of the diffuse γ-ray emission from the Galaxy suggest the value

$$D = D_{28} \times 10^{28} [E_{\rm CR}/4\ {\rm GeV}]^{-\delta}\ {\rm cm}^2/{\rm s}, \qquad (1)$$

with an uncertainty of the prefactor D_{28} by up to a factor of $\simeq 3$ and with the slope $\delta = 0.4 \pm 0.1$ [3]. CRs released from a source some T_s years ago are now filling a volume of size [4]

$$r_s \simeq 2\sqrt{DT_s} \simeq 80 D_{28}^{1/2} \left[\frac{T_s}{10\ {\rm kyr}}\right]^{1/2} \left[\frac{E_{\rm CR}}{1\ {\rm TeV}}\right]^{\delta/2} {\rm pc}. \qquad (2)$$

The average density of ISM on this distance scale is $n_{\rm ISM} \sim 1\ {\rm cm}^3$ [18]. The typical interaction time of CRs propagating through the ISM is

$$t_{pp} = (c\sigma_{pp} n_{\rm ISM})^{-1} \simeq 3 \times 10^7 \left[\frac{n_{\rm ISM}}{1\ {\rm cm}^{-3}}\right]^{-1} {\rm yr}, \qquad (3)$$

where we adopt an estimate $\sigma_{pp} \simeq 4 \times 10^{-26}\ {\rm cm}^2$ for the cross section of inelastic proton-proton collisions for the TeV CRs [19].

CR interactions with ISM inside a region of the size r_s lead to extended γ-ray (and neutrino) emission from the entire CR filled volume. The γ-ray luminosity can be readily estimated taking into account that each source must release some $E_s \sim 3 \times 10^{50} [\mathcal{R}_{SN}/10^{-2}\ {\rm yr}]^{-1}$ erg in the form of CRs, where $\mathcal{R}_{SN}$ is the rate of CR injection events in the Galaxy. This leads to the estimate

$$L_\gamma \sim \frac{\kappa E_s}{t_{pp}} \sim 2 \times 10^{34} \left[\frac{\kappa}{0.2}\right] \left[\frac{E_s}{10^{50}\ {\rm erg}}\right] \left[\frac{n_{\rm ISM}}{1\ {\rm cm}^{-3}}\right] {\rm erg/s}, \qquad (4)$$

where $\kappa \sim 0.2$ is a typical fraction of the CR energy deposited in the γ-rays. Note that this luminosity depends only on the average density of the ISM. It is largely independent of the physical parameters of the source itself. The only source parameter which is fixed by the general energy requirement on the Galactic CR sources is the released energy in the form of CRs, E_s. The estimate of L_γ in Eq. (4) is uncertain by at least a factor of $\sim$3 [1,2]. This includes the uncertainty of the estimate of the typical energy output per source, E_s, which depends on the lifetime of CRs in the Galactic disk, the thickness of the disk, and the rate of the injection events (with large uncertainties in all the three factors). Besides, the estimate of L_γ is energy dependent, due to the energy dependence of the source power and of the CR lifetime in the Galactic disk.

III. EXTENDED VHE γ-RAY EMISSION AROUND CR SOURCES

The luminosity level given in Eq. (4) is high enough for the γ-ray emission to be detectable with existing space- and ground-based γ-ray telescopes. The main difficulty for the detection of extended emission around the individual CR sources is that it has to be identified on top of the diffuse γ-ray emission from the Galaxy [20].

In the energy band 0.1–1 GeV this diffuse emission appears as a collective emission from a very large number of extended sources. Possible emission around individual sources can not be identified. The difficulty for the identification of individual sources is, in fact, the problem of the source confusion. The 0.1–1 GeV γ-rays are produced by the CRs with energies in the $E_{\rm CR} \sim$ 1–10 GeV range. In

this energy range the size of the extended emission region around the source reaches the $\gtrsim 100$ pc scale in $\sim 10^5$ yr [see Eq. (2)]. Assuming the supernova rate of $\mathcal{R}_{SN} \sim 10^{-2}\ \mathrm{yr}^{-1}$, one finds that the 100 pc scale regions around some $N_s \sim 10^3/D_{28}(\mathcal{R}_{SN}/10^{-2}\ \mathrm{yr}^{-1})$ sources are currently filling the Galactic disk. The density of the sources is $\rho_s \sim N_s/V_{\mathrm{disk}} \sim 3\ \mathrm{kpc}^{-3}$, where $V \simeq 2\pi(10\,\mathrm{kpc})^2 H_{\mathrm{disk}} \sim 300\,\mathrm{kpc}^3$ is the volume of the Galactic disk. This implies typical distance between the centers of the extended emission, $\sim$700 pc, so that in any direction in the inner Galaxy one would find on average several extended sources within several kiloparsec distance are superimposed on each other. An additional difficulty is the large size of the point-spread function (PSF) of the LAT in this energy band [17].

The number of sources surrounded by the extended emission decreases with the increasing energy. At energies $E_\gamma \gtrsim 100$ GeV (the CR energies in the TeV range), the extended emission region size reaches the 100 pc in $\sim$10 kyr [see Eq. (2)]. Some $\lesssim 100$ sources are currently surrounded by the 100 pc scale extended emission, so that the density of the sources decreases down to $\sim 0.3\ \mathrm{kpc}^{-3}$. The typical source-to-source distance is $\sim$1.5 kpc so that there is no overlap. Relatively compact and bright extended γ-ray emission around nearby and recent CR sources should start to be identifiable in the data.

A source which released CRs some T_s yr ago is surrounded by extended emission of the angular size

$$\theta_s \sim \frac{r_s}{R_s} \simeq 0.8^\circ D_{28}^{1/2}\left[\frac{R_s}{5\ \mathrm{kpc}}\right]^{-1}\left[\frac{T_s}{10\ \mathrm{kyr}}\right]^{1/2}\left[\frac{E_{\mathrm{CR}}}{1\ \mathrm{TeV}}\right]^{0.2}, \tag{5}$$

where R_s is the distance to the source. The expected γ-ray flux is

$$F_s = \frac{L_\gamma}{4\pi R_s^2} \simeq 10^{-11}\left[\frac{R_s}{5\ \mathrm{kpc}}\right]^{-2}\left[\frac{n_{\mathrm{ISM}}}{1\ \mathrm{cm}^{-3}}\right]\left[\frac{\kappa}{0.2}\right]\frac{\mathrm{erg}}{\mathrm{cm}^2\,\mathrm{s}}. \tag{6}$$

A reasonable task is to search for the relatively compact γ-ray emission around the TeV CR sources of the age $T_s \sim 10^4$ yr on top of the diffuse background. Up to

$$N_s \sim \rho_s \pi R_s^2/2 \sim 12 D_{28}^{-1}\left[\frac{R_s}{5\ \mathrm{kpc}}\right]^2\left[\frac{T_s}{10\ \mathrm{kyr}}\right]^{1/2}\left[\frac{\mathcal{R}_{SN}}{1/100\ \mathrm{yr}}\right] \tag{7}$$

degree-scale extended sources could be detectable within the $\sim$5 kpc distance in the inner Galaxy where the density of the ISM is high enough to provide the required luminosity level.

Detection/nondetection of the degree-scale sources at the flux level given by Eq. (6) provides a test for the supernova scenario of CR production. Indeed, nondetection would rule out the possibility that the CRs are injected in portions of $\sim 10^{50}$ erg once every $\sim$100 yr and would instead point to a scenario where the CRs are injected continuously throughout the Galaxy, as it is expected in the scenario of cosmic ray production via acceleration at multiple shocks formed by the stellar wind bubbles and supernova explosions in the star-forming regions. It is, however, worth mentioning that in this scenario the degree-scale extended emission might still originate from the individual most active superbubbles which are currently accelerating cosmic rays.

IV. SEARCH FOR THE DEGREE-SCALE SOURCES IN THE LAT DATA

The results obtained in the previous section suggest that the nearby and relatively recent sources of TeV CRs should reveal themselves though the degree-scale extended γ-ray emission. The expected flux level (6) is high enough so that the LAT sensitivity at 100 GeV is sufficient for the source detection.

We have analyzed the data collected in the period between August 2008 and October 2011 using the FERMI SCIENCE TOOLS.[1] The LAT event lists were filtered using *gtselect* tool and only "superclean" γ-ray events (`evtclass = 4`) with energies above 100 GeV arriving at zenith angles $\theta_z < 100^\circ$ were retained for the analysis. To identify the extended sources of the size $\theta_s \lesssim 1^\circ$ in the LAT data above 100 GeV we have used the minimal spanning tree (MST) method [21–23]. In this method photons separated by angular distances smaller then a predefined value θ_{max} are considered as belonging to a "cluster" or "tree." Pointlike or extended sources could be found on top of the diffuse background as trees with large enough number of photons. Significance of the source detection can be estimated via comparison of the real data with Monte Carlo (MC) simulations.

To increase the sensitivity of the MST method for the search of extended γ-ray sources we took θ_{max} in the range $0.3^\circ < \theta_{\mathrm{max}} < 0.5^\circ$, which is larger than the size of the PSF of the LAT at the energies above 100 GeV. In this respect the MST procedure is different from that used in the Ref. [23]. Close to the Galactic plane, the level of diffuse sky background depends on the source location. The increase of θ_{max} leads to the increase of the chance coincidence probability of association of diffuse background photons with a tree. To estimate the background at each source location we used MC simulations which generate the background maps from the real data by changing the sky photon coordinates (l, b). In these MC simulations the Galactic latitude of the photons was left unchanged, while the longitude was randomly redistributed within $\Delta l = \pm 10^\circ$ around the real photon position.

We measure the extension of the sources by comparing the photon distribution around the source position with the PSF. To estimate the LAT PSF at $E > 100$ GeV we took

[1] http://fermi.gsfc.nasa.gov/ssc/data/analysis/

1319 sources from second Fermi catalog [24] with $|b| > 10°$ and calculated flux around them as function of angle. Results of this calculation are shown in the Fig. 1 separately for front and back photons. The 90% containment radius is $\theta_{90,f} = 0.14°$ for front photons and $\theta_{90,b} = 0.33°$ for back photons. We consider the sources for which 90% of $E > 100$ GeV events are within $\theta_{90,f}$, $\theta_{90,b}$ as point sources, while other sources are considered as extended. We remove photons associated to the point sources in the search for event clusters associated to extended sources.

To identify point sources, we search for the correlation of the photon arrival directions with the positions of the sources from the two-year Fermi catalogue [24], in a way similar to the one used in the Ref. [25] for the search of the extragalactic VHE γ-ray sources. The list of point sources found above 3σ significance threshold is presented in the Table I. In this table we give the name of source in 2FGL catalog, galactic coordinates l and b, the number of photons within 90% C.L. angle from source, its significance calculated using binomial probability, the type of the source, and its alternative name for the identified sources. We also looked for the point sources with the MST method with photon separation $\theta = 0.2°$. This method does not rely on the predefined source catalogue. The search with the MST method did not result in additional point sources which are not associated to the known 2FGL source.

Ten out of 14 point sources listed in Table I are known VHE γ-ray sources. Four sources are new detections: VCS (J0110 + 5805), 2FGL (J1030.4 − 6015), PSR (J1124 − 5916), and AT20G 9J160350 − 49). Five out of 14 sources are extragalactic sources found at low Galactic latitudes. Three sources are of unknown type. Other sources are known brightest Galactic γ-ray sources. All

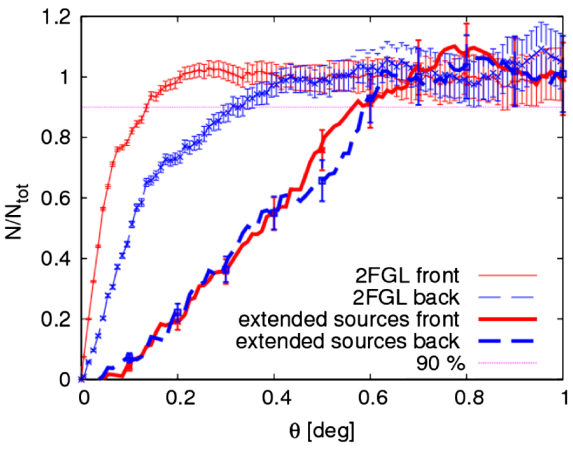

FIG. 1 (color online). Cumulative photon distribution as function of angle from the source position in the energy band above 100 GeV. Thin lines are for PSF around extragalactic Fermi sources. Thick lines are photon distribution for the Galactic sources from Table II. The solid line is for front photons and the dashed line is for back photons. Error bars indicate the uncertainty due to background fluctuations.

the photons associated to the point sources listed in Table I are subtracted from the overall photon list used in the search of extended sources.

The list of extended sources found using the MST method is given in Table II. To reduce the amount of false trees formed by fluctuations of the background, we considered only trees with known counterparts from the TeVCat catalogue of VHE γ-ray sources[2] for the source in the inner Galaxy ($-60° < l < 60°$). After imposing such a requirement, two out of 14 extended sources in the inner Galaxy are expected to be due to background fluctuations.

Figure 2 shows the LAT count map in the energy range 0.1–0.4 TeV smoothed with 0.5° Gaussian. The positions of the sources listed in Tables I and II are shown on the map.

The average radial brightness profile of the extended sources from Table II is shown in Fig. 1. One can see that the profile is clearly different from the LAT PSF. The cumulative photon distribution traces source photons up to $\theta \sim 0.6°$. The angular sizes of the sources reported in the Table II are generally larger than the sizes reported in the HESS survey [26]. This difference might be attributed to the difference of the observation techniques used by the LAT and HESS telescopes.

V. DETAILS FOR INDIVIDUAL EXTENDED GALACTIC VHE γ-RAY SOURCES

The estimates of the Sec. III show that recent sources of TeV CRs should be surrounded by degree-scale extended VHE γ-ray emission with the flux in excess of $\sim 10^{-11}$ erg/(cm^2 s). The sources listed in Table II satisfy this requirement. This means that they could trace recent injections of CRs in the Galaxy. In this section we investigate the nature of CR accelerators which might power the observed extended emission in each individual source.

A. $(l, b) = (8.15, -0.14)$

This excess is associated to HESS source HESS J1804 − 216, see Fig. 3. The size of the LAT event cluster associated to the source is clearly larger than the extent of the source measured by HESS. The original discovery paper by HESS [26] suggests a PWN interpretation of the source associating it to a Vela-like pulsar PSR J1800 − 21 [27,28] with spin-down age $T_s \simeq 1.7 \times 10^4$ yr situated at the distance $D \simeq 3$–4 kpc [29].

Alternatively, an association with a shell-type SNR could be considered. The SNR in question is G8.7–0.1, which is a relatively young (10^4 yr) and nearby SNR visible in the 0.1–100 GeV energy band [30]. Possible association of G8.7-0.1 with PSR J1800 − 21 is considered

[2]http://tevcat.uchicago.edu

TABLE I. List of pointlike VHE sources found at the positions of known Fermi sources. l, b are source coordinates, N_{ph} is the number of photons within the 90% containment radius of the PSF, and P is the chance coincidence probability for the event cluster to be a background fluctuation. Notations in the column "type" are PWN, supernova remnant with compact central object (SNR + CCO), blazar (BLZ), active galactic nucleus unknown type (AGU), and γ-ray loud binary (GRLB). Previously reported VHE γ-ray sources are marked in bold. Other sources are new detections in the VHE band.

	2FGL	l	b	N_{ph}	P	Type	Name
1	1837.3 − 0700c	25.09	−0.08	4	1.e − 4		**HESS J1837−069**
2	J2001.1 + 4352	79.06	−7.12	2	1.e − 3	BLZ	**MAGIC J2001+435**
3	J2323.4 + 5849	111.74	−2.11	2	1.e − 3	SNR	**Cas A**
4	J2347.0 + 5142	112.88	−9.90	4	6.e − 8	BLZ	**1ES 2344+514**
5	J0035.8 + 5951	120.97	−2.96	5	4.e − 8	BLZ	**1ES 0033+595**
6	J0110.3 + 6805	124.70	5.29	2	6.e − 4		VCS J0110 + 6805
7	J0240.5 + 6113	135.67	1.08	4	2.e − 6	GRLB	**LS I+ 303**
8	J0521.7 + 2113	183.6	−8.70	4	2.e − 5	AGU	**VCS J0521+2112**
9	J0534.5 + 2201	184.55	−5.78	28	0	PWN	**Crab**
10	J0617.2 + 2234e	189.05	3.03	4	7.e − 5	SNR + CCO	**IC443**
11	J0648.9 + 1516	198.99	6.35	4	4.e − 7	AGU	**VER J0648−152**
12	J1030.4 − 6015	286.28	−2.03	2	1.e − 3		
13	J1124.6 − 5913	292.2	−2.03	2	1.e − 3	PWN	PSR J1124 − 5916
14	J1603.8 − 4904	332.15	2.56	5	5.e − 7		AT20G J160350 − 49

(see e.g. [27]) based on the proximity of the two objects in space and similar age.

B. $(l, b) = (17.58, -0.14)$ and $(l, b) = (16.74, -1.79)$

This extended emission region includes the HESS source HESS J1825 − 137, which is identified with the pulsar PSR B1823 − 13 [31,32]; see Fig. 4. Similarly to PSR J1800 − 21, this is a relatively nearby (4 kpc) and young (20 kyr) pulsar [29].

The extended radio source, possibly a supernova remnant, G 17.4 − 0.1 [33], is found within the source extension, so that relation of the extended emission to a

TABLE II. List of extended sources found in the MST analysis. θ_{50}, θ_{90} are the radii within which 50% and 90% of the tree photons are contained. N_{ph} is the background subtracted number of photons in the tree. P_{90} is the chance coincidence probability of background fluctuation which would have N_{ph} photons within a circle of the radius θ_{90}. F is the source flux in units of 10^{-11} erg/cm^2 s. SNR and PSR columns give the names of supernova remnants and/or pulsars suggested to be associated to the source. R_s and T_s are the source age (in the units of 10^4 yr) and distance (in kpc).

	l	b	θ_{50}	θ_{90}	P_{90}	N_{ph}	F	Comments	SNR	PSR	R_s	T_s
1	8.15	−0.14	0.47	0.65	1.e − 5	12	4.6 ± 1.3	HESS 1804 − 216	W30	B1800 − 21	3.9	1.6
2	16.74	−1.79	0.46	0.83	1.e − 6	12		LS 5039				
3	17.58	−0.14	0.6	1. 0	1.e − 3	13	5.2 ± 1.4	HESS J1825 − 137		B1823 − 13	4.1	2.1
4	23.32	−0.16	0.5	0.6	2.e − 2	8	3.4 ± 1.2	HESS J1834 − 087	W41	CXOU J183434.9 − 084443	4	∼10
										B1830 − 08?		3.5
5	25.21	−0.16	0.43	0.58	1.e − 5	15	6.4 ± 1.5	HESS J1837 − 069		J1838 − 0655		2.3
6	26.87	−0.12	0.39	0.54	2.e − 4	11	4.6 ± 1.4	HESS J1841 − 055		J1841 − 0524	4.9	3.0
7	36.20	0.02	0.23	0.37	1.e − 6	11	4.6 ± 1.4	HESS J1857 + 026		J1856 + 0245	10.3	2.0
8	78.09	2.54	0.33	0.38	1.e − 5	7	2.3 ± 0.9	VER J2019 + 407	γCyg	J2021 + 4026		7.7
9	284.32	−0.57	0.32	0.42	7.e − 3	4	1.3 ± 0.7	Westerlund 2		J1023 − 5746		0.5
10	287.12	−0.80	0.46	0.74	2.e − 4	9	2.9 ± 1.0	Near Eta Car				
11	313.56	0.11	0.2	0.32	8.e − 6	8	2.6 ± 1.0	Kookaburra		J1420 − 6048	7.7	1.3
12	331.66	−0.58	0.27	0.64	7.e − 4	11	3.7 ± 1.1	HESS 1614 − 518		J1614 − 5144		
13	332.57	−0.18	0.34	0.63	1.e − 3	10	3.3 ± 1.0	HESS J1616 − 508		J1617 − 5055	6.5	0.8
14	336.25	0.04	0.37	0.59	1.e − 6	16	5.4 ± 1.3	HESS J1632 − 478		J1632 − 4757	7.0	24
15	339.56	−0.79	0.37	0.72	3.e − 3	10	3.4 ± 1.0	Westerlund 1		J1648 − 4611	5.7	11
16	344.90	0.23	0.72	1.05	3.e − 2	8	2.8 ± 1.1	HESS J1702 − 420		J1702 − 4128?	5.2	5.5
17	346.20	−0.31	0.37	0.57	1.e − 2	7	2.7 ± 1.0	HESS 1708 − 410		J1706 − 4009?	3.8	0.9
18	358.06	−0.54	0.57	0.63	1.e − 4	10	3.7 ± 1.2	HESS J1745 − 303				

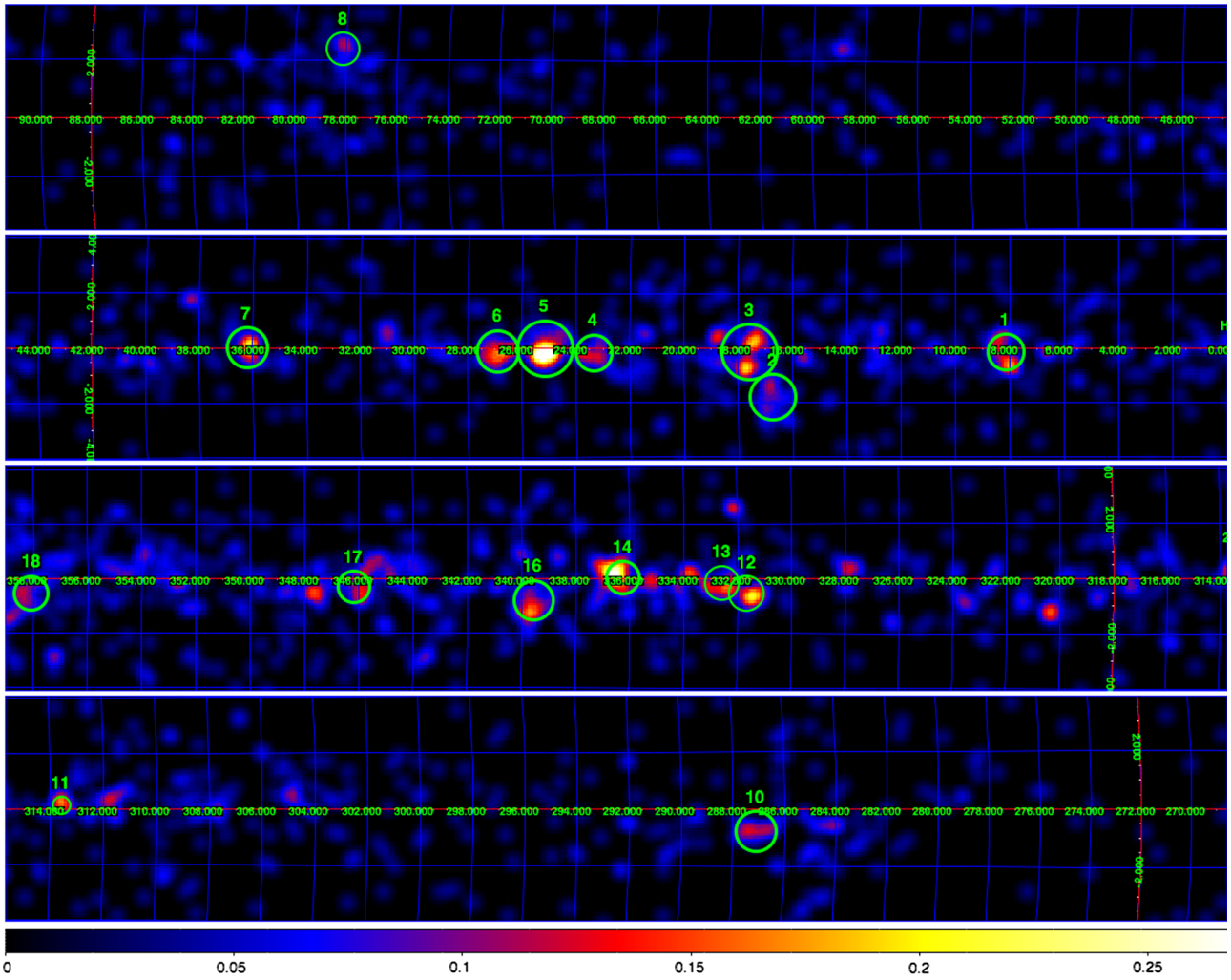

FIG. 2 (color online). LAT count map of the inner Galaxy in the 100–400 GeV band smoothed with a 0.5° Gaussian. VHE γ-ray sources from Table II are shown by green circles.

shell-like SNR could not be ruled out. Lack of basic information on G 17.4 − 0.1 (age, distance) makes the analysis of association of the observed extended emission to G 17.4 − 0.1 impossible.

Immediately adjacent to the extended source around HESS J1825 − 137, there is an extended emission which includes a γ-ray loud binary LS 5039 (Fig. 4). It is not clear if this source is just a further extension of a brighter HESS J1825 − 137, or it is an independent source. The relation of this source to LS 5039 is also not evident.

Energy-dependent morphology of HESS J1825 − 137 was studied in detail in the Ref. [32]. Detailed observations by HESS have revealed a more compact emission region of the size ∼0.3° at the highest energies on top of a more extended degree-scale emission at the energies of several hundred GeV. Suzaku observations of the HESS J1825 − 137 region reveal an extended x-ray emission associated to the central more compact 0.3° source, but not to the extended degree-scale source [34]. The x-ray emission detected by Suzaku could be consistently interpreted as synchrotron emission from electrons in the PWN of PSR B1823 − 13. The absence of x-ray emission from the degree-scale source might indicate that the degree-scale γ-ray emission is due to CR interactions.

C. $(l, b) = (23.32, -0.16)$, $(25.21, -0.16)$ and $(26.87, -0.12)$

The event clusters associated to these three adjacent excesses merge into one extended emission region along the Galactic plane, in which the central source, the cluster at $(l, b) = (25.21 - 0.16)$, dominates. This central source is associated to the HESS source HESS J1837 − 069 identified with a PWN of the pulsar PSR J1838 − 0655 [35,36], which has the spin-down age of ∼22 kyr [29].

The side sources are also associated to the HESS sources HESS J1834 − 087 and HESS J1841 − 055 (Fig. 5). The most probable low-energy counterpart of HESS J1834 − 087 is the SNR W41, which contains a central PWN-like object CXOU J183434.9 − 084443 [37,38]. Reference [39] provides an estimate of the age of this

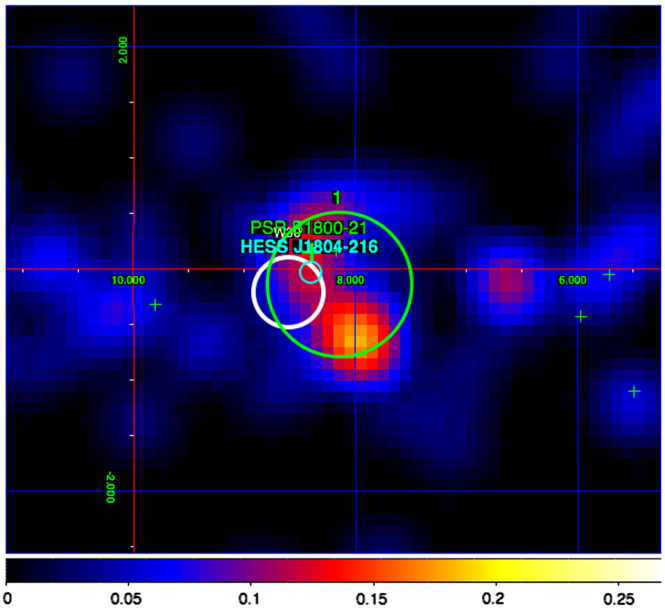

FIG. 3 (color online). Sky region around extended source at $(l, b) = 8.15, -0.14$). The white circle marks the position of 2FGL extended source associated to supernova remnant W30.

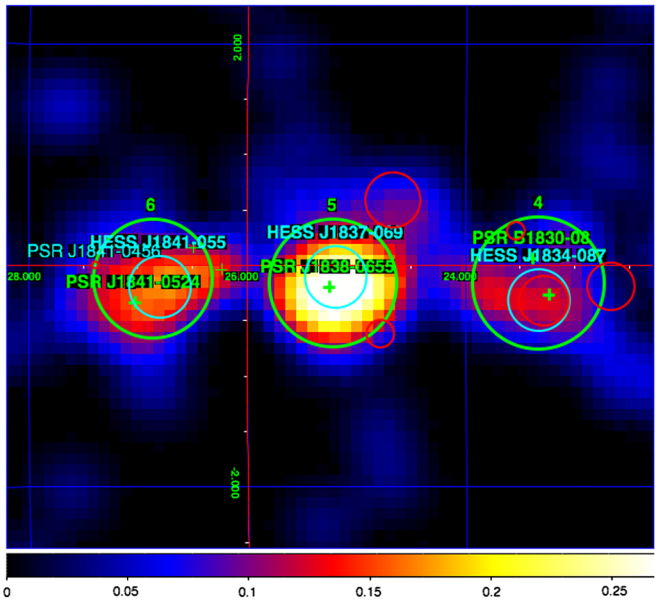

FIG. 5 (color online). Sky region around extended sources at $(l, b) = (23.32, -0.16)$, $(25.21, -0.16)$ and $(26.87, -0.12)$. The green cross inside HESS J1834 − 087 marks the position of CXOU J183434.9 − 084443. Red circles show positions and sizes of SNRs from the Green catalogue [42].

SNR, $T_s \sim 10$ kyr. The extension of the cluster of events associated to HESS J1834 − 087 is, however, larger than the size of the HESS source. Within this extension another relatively young pulsar is present, PSR B1830 − 08 (see Fig. 5), which somewhat younger, $T_s \simeq 30$ kyr.

The source associated to the HESS J1841 − 055 does not have a shell-like SNR candidates within its extension. At the same time, a young nearby pulsar PSR J1841 − 0524 of spin-down age $T_s \simeq 30$ kyr [29] is situated in the center of the source. This pulsar could be considered as a possible low energy counterpart of the extended γ-ray source.

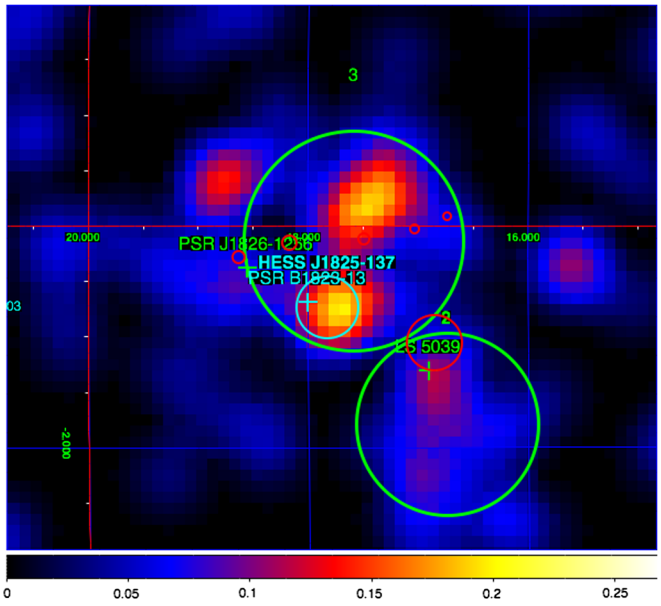

FIG. 4 (color online). Sky region around extended source at $(l, b) = 17.58, -0.14$). Red circles show positions and sizes of SNRs from the Green catalogue [42].

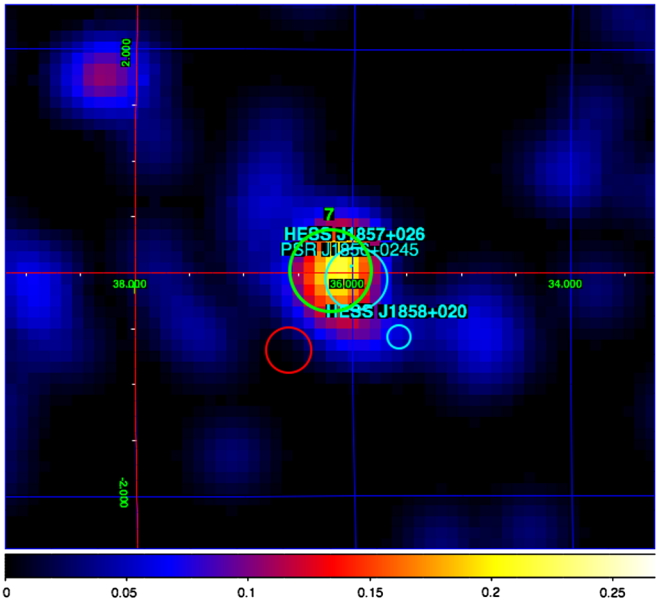

FIG. 6 (color online). Sky region around extended source at $(l, b) = (36.20, 0.02)$. The red circle shows position and size of a SNR from the Green catalogue [42].

D. $(l, b) = (36.20, 0.02)$

This extended source is spatially coincident with HESS source HESS J1857 + 026 and is identified with a PWN of PSR J1856 + 0245 [40,41] of spin-down age $T_s \simeq 20$ kyr. No shell-like supernova remnant from the Green catalogue [42] is found within the source extent (see Fig. 6). The size of event cluster associated with the source is much larger than the reported size of the HESS source (see Fig. 6). The source is elongated in the direction of another HESS source, HESS J1858 + 020.

E. $(l, b) = (78.09, 2.54)$

This source is a part of extended emission from the PSR J2021 + 4026—γCygni PWN + SNR system. The centroid of extended emission is displaced from the pulsar position, but the emission still comes from within the SNR boundary (Fig. 7), so that it is not the extended emission from the CRs escaping into the ISM. Taking into account the age of the SNR, $T_s \simeq 80$ kyr, and its proximity $R_s \simeq 1.5$ kpc [43] one could find that the expected size of the extended emission from the escaping CRs is $\theta_s \simeq 5^\circ$ (5), i.e. it is expected to cover the entire Cygnus region.

GeV band extended emission on the angular scale $\sim 5^\circ$ from the sky region immediately adjacent to the γCygni source was recently discussed in the Ref. [11]. This reference attributes the extended emission to the interactions of CRs in the ISM. Although the possibility of relation of this extended emission to γCygni is mentioned in this reference, an alternative possibility for the origin of CRs interacting in the ISM is considered, based on the spatial displacement of the source from the γCygni position.

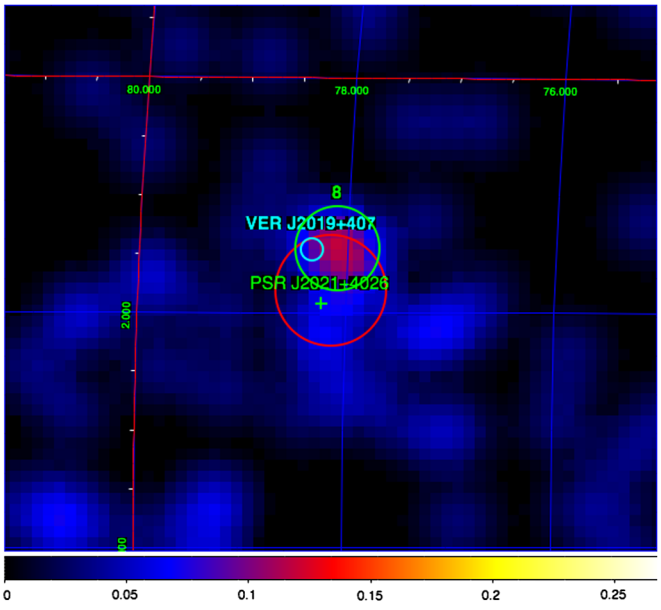

FIG. 7 (color online). Sky region around extended source at $(l, b) = (78.09, 2.54)$. The red circle shows the extent of γCygni SNR.

The scenario favored in the Ref. [11] is injection of cosmic rays via acceleration at multiple shocks formed by stellar wind bubbles in the OB associations in the Cygnus region, which form the Cygnus superbubble.

We notice that in principle the displacement of the extended emission from the *possible* primary source position (pulsar) is expected, because of the presence of the ordered component of Galactic magnetic field. Ordered magnetic field introduces anisotropy in the CR diffusion from the source, so that the extended emission produced by CRs escaping from the source is not expected to be symmetrically distributed around the source position. Additional asymmetry could be introduced by spatial variations of the ISM density.

It is also worth noticing that, contrary to the low-energy (GeV) emission, the maximum of the extended emission in the VHE band is spatially coincident with the γCygni supernova remnant associated to PSR J2021 + 4026. This suggests that the higher energy (TeV) and lower energy (1–10 GeV) might be produced at different locations, via different acceleration mechanisms.

F. $(l, b) = (284.32, -0.57)$ and near Eta Car

The excess at $(l, b) = (284.32 - 0.57)$ is positionally coincident with the HESS source HESS 1023 − 575 identified as a PWN of PSR J1023 − 5746 (previously associated with Westerlund 2 cluster) [44]. The pulsar is relatively young, $T_s \simeq 5$ kyr. Absence of the radio emission does not allow the measurement of the distance based on the dispersion measure [29]. No shell-like supernova remnant from the Green catalogue is visible within the source extension.

No obvious counterpart candidates could be found within the extent of the emission region adjacent to the Eta Car (see Fig. 8): no known pulsars or shell-like SNRs. The nature of this excess requires further investigation. The emission from this sky region comes from the direction tangential to the Carina-Sagittarius arm of the Galaxy. The enhancement of the 100 GeV emission might, in principle, be an enhancement of Galactic diffuse emission due to the projection effect.

G. $(l, b) = (313.56, 0.11)$

The extended source at $(l, b) = (313.56, 0.11)$ is spatially coincident with the known HESS source at the Kookaburra PWN around PSR J1420 − 6048 of the age 13 kyr situated at the distance 7.7 kpc [29]; see Fig. 9.

H. $(l, b) = (331.66, -0.58)$, $(l, b) = (332.57, -0.18)$ and $(l, b) = (336.56, 0.04)$

The three excesses are close to each other so that the event clusters associated to these three sources merge into a single extended emission region along the Galactic plane. The excesses could be identified with known HESS

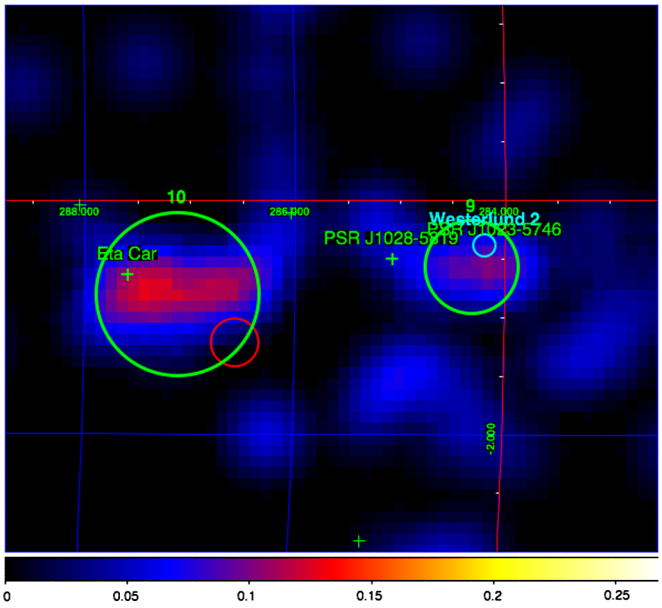

FIG. 8 (color online). Sky region around extended source at $(l, b) = (284.32, -0.57)$ and near Eta Car. Red circle shows position and size of a SNR from the Green catalogue [42].

sources: HESS J1614 − 518, HESS J1616 − 508, and HESS J1632 − 4757 (see Fig. 10).

The source at the position of HESS J1614 − 518 does not have any known pulsars or SNRs within its extent. The direction toward this source is tangent to the Norma arm of the Galaxy. Similarly to the case of the Scrutum-Centaurus arm, enhancement of the matter density in the arm and projection effects might be responsible for the enhanced VHE γ-ray flux from this direction.

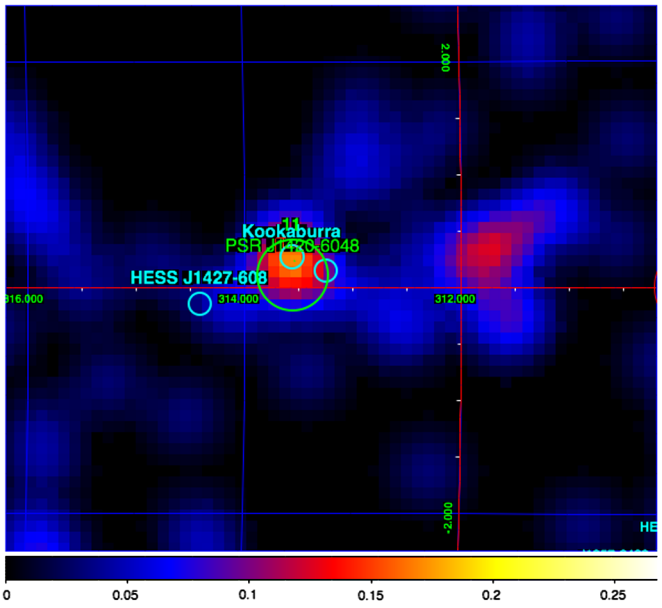

FIG. 9 (color online). Sky region around extended source around $(l, b) = (313.56, 0.11)$.

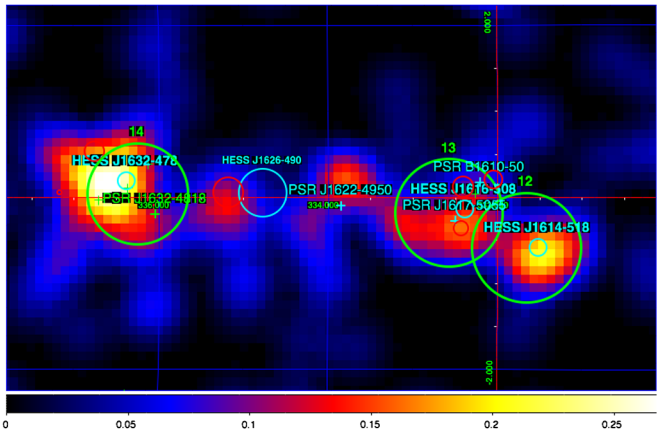

FIG. 10 (color online). Sky region around extended source around $(l, b) = (331.66, -0.58)$, $(l, b) = (332.57, -0.18)$, $(l, b) = (334.97, -0.26)$ and $(l, b) = (336.56, 0.04)$. Red circles show positions and sizes of SNRs from the Green catalogue [42].

HESS J1616 − 508 is most probably associated to the PWN of PSR J1617 − 5055 [45] of the age $T_s \simeq 8$ kyr [29], although several shell-like SNRs are adjacent to the HESS source position and are within the extent of the LAT event cluster at $(l, b) = (332.57, -0.18)$ (see Fig. 10).

The event cluster at the position of HESS J1632 − 478 is the brightest excess in this source group. The maximum of excess is at the position of the pulsar PSR J1632 − 4757 and Ref. [46] associates the source to the pulsar. In this case the age of the supernova associated to the source is $T_s \simeq 24$ kyr. Several other pulsars and SNRs, as well as another HESS source, HESS J1634 − 472, are found at the periphery of the source (see Fig. 10). It is possible that the overall emission from this bright excess is composed of contributions from several sources.

I. Source at $(l, b) = (339.56, -0.79)$

Excess at this position coincides with the HESS source in the direction of Westerlund 1 stellar cluster. The LAT event cluster associated to the source is more extended than the HESS source toward the position of the LAT pulsar PSR J1648 − 4611 (Fig. 11). This is a $T_s \simeq 100$ kyr pulsar situated in the Norma arm of the Galaxy at the distance $R_s \simeq 5$ kpc.

J. $(l, b) = (344.90, 0.23)$ and $(l, b) = (346.20, -0.31)$

The LAT event cluster in this direction extends along the Galactic plane between three HESS sources, HESS J1702 − 420, HESS J1708 − 410 (Fig. 12). Several shell-like SNR and pulsar wind nebulae (PWNe) are found within the source extent, so that no "natural" counterpart candidates could be identified. Maximum of the excess at 100 GeV is at HESS J1708 − 410, but at slightly lower energies the maximum shifts toward HESS J1702 − 420, close to the pulsar PSR J1702 − 4128, so that the source morphology is energy-dependent. This pulsar has the age 55 kyr and is situated at

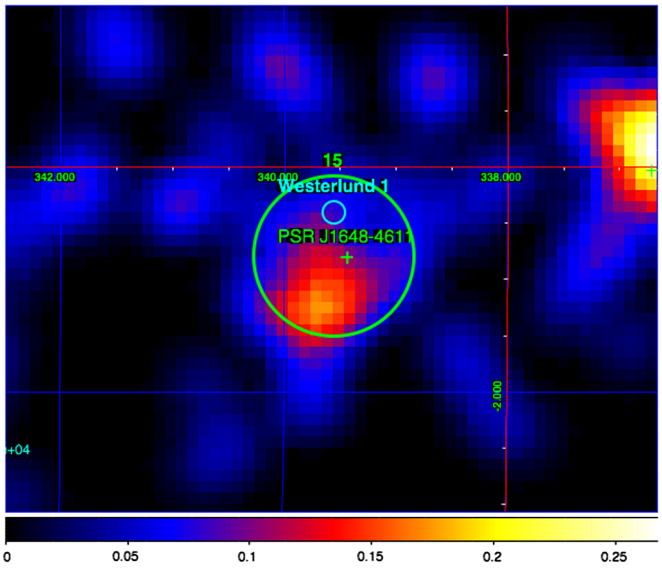

FIG. 11 (color online). Sky region around extended source at $(l, b) = (339.56, -0.79)$.

the distance $\simeq 5$ kpc [29]. Another pulsar, PSR J1706 − 4009, is situated within the extent of the event cluster at $(l, b) = (346.20, -0.31)$. This pulsar is situated at the distance 3.8 kpc and has the spin-down age 9 kyr [29].

K. Source at $(l, b) = (358.06, -0.54)$

This excess is at the position of the HESS source HESS J1745 − 303, but has a much larger size than the HESS source. Several pulsars and shell-type SNRs are found within the source extension so that no obvious counterpart candidate could be singled out; see Fig. 13.

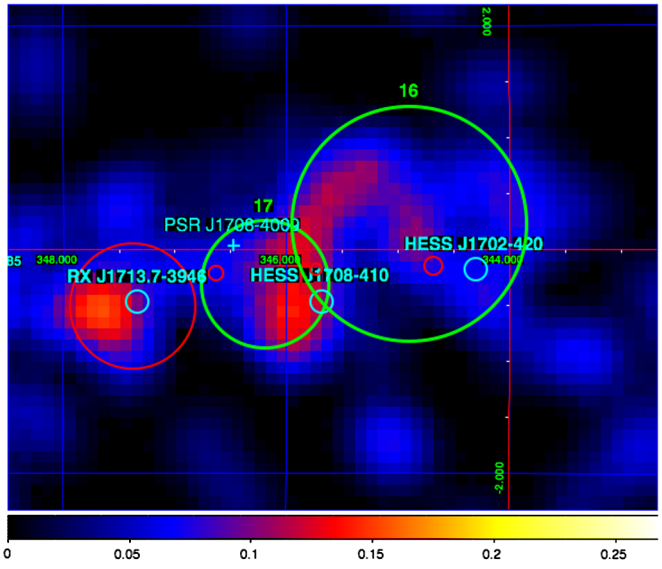

FIG. 12 (color online). Sky region around extended sources at $(l, b) = (344.90, 0.23)$ and $(l, b) = (346.20, -0.31)$. Red circles show positions and sizes of SNRs from the Green catalogue [42].

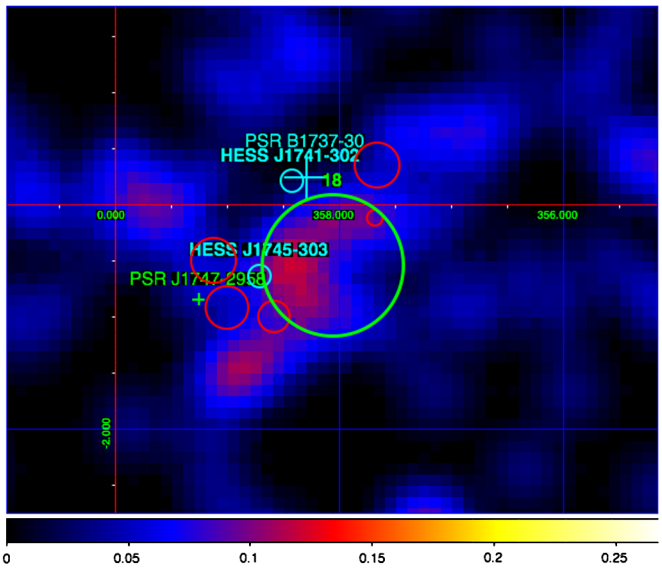

FIG. 13 (color online). Sky region around extended source at $(l, b) = (358.06, -0.54)$. Red circles show positions and sizes of SNRs from the Green catalogue [42].

VI. THE NATURE OF EXTENDED SOURCES

The overall number of extended 100 GeV γ-ray sources at the flux level in excess of 10^{-11} erg/cm^2 s is consistent with the expected number of the regions of degree-scale extended emission around recent TeV CR sources in the scenario in which CRs are injected in portions of $\sim 10^{50}$ erg rather than continuously all over the Galaxy (see Secs. II and III). The source sizes are also consistent with an assumption that the extended emission is produced by high-energy particles diffusing into the ISM. Fifteen out of the 18 extended sources listed in the Table II are possibly or clearly associated with pulsars of the age $T_s \lesssim 30$ kyr. This is consistent with the hypothesis that TeV CRs are injected by supernova-related phenomena. Indeed, majority of the core collapse supernova (more than 75%) in the Galaxy are expected to result in production of the neutron star [47]. Most of the collapsing massive stars are rotating, so that significant fraction of the newborn neutron stars are expected to be visible as pulsars [48].

An essential element of the supernova scenario for the origin of CRs is that a significant part of supernovae (rather than just a small fraction of them) should inject some 10^{50} erg of CRs in the interstellar medium. The assumption that every supernova injects $\sim 10^{50}$ erg in CRs implies that the 100 pc scale extended VHE γ-ray emission regions should exist around nearly all the relatively recent (30 kyr) supernovae. Calculations of the previous sections suggest that extended emission regions situated at the distance $R_s \lesssim 5$ kpc should be detectable at the flux level in excess of 10^{-11} erg/cm^2 s.

The sensitivity of LAT in the $E > 100$ GeV energy range is only marginally sufficient for detection of

degree-size sources with fluxes 10^{-11} erg/cm^2 s. In fact, all the sources listed in Table II have slightly higher fluxes. This means that, in principle, some extended emission regions around the nearby TeV CR sources of the age $T \lesssim 30$ kyr might have escaped detection by LAT. At the same time, their flux level might be above the sensitivity of the ground-based γ-ray telescopes. To verify this conjecture, we compiled a list of all known pulsars with the spin-down age shorter than 30 kyr using the ATNF pulsar catalogue [29]. As it is explained above, such pulsars could be used as tracers of recent supernova explosions. Figure 14 shows the locations of the pulsars in the plane of the Galaxy. There are 56 such pulsars at the distances smaller than 20 kpc. Some 29 of them are found within 0.5 degrees from the known VHE γ-ray sources. The list the pulsars found in vicinity of known VHE sources, which are not detected in the MST analysis of LAT data is given in Table III. In fact, a large fraction of the sources listed in Table III are associated with 100 GeV γ-ray event clusters in LAT, but with the event statistics below the threshold adopted in our analysis.

The positions of the pulsars associated with the brightest extended VHE γ-ray sources listed in Table II are marked by magenta boxes in Fig. 14. One could notice that most of the sources are situated in the Norma arm of the Galaxy, which is $\sim$5 kpc away from the Sun. The fact that the extended sources in the Norma arm appear brighter than the extended emission around closer CR sources might look surprising at the first sight. However, the Norma arm is a special region of the Galaxy with the highest star formation rate [49]. High star formation rate is associated to the increased matter density in the arm (presence of numerous molecular clouds), which boosts the VHE γ-ray luminosity of the extended emission. Positions of the pulsar-associated extended or point sources which are below the LAT sensitivity above 100 GeV, but possibly associated to the VHE γ-ray emission are marked by the blue circles in Fig. 14.

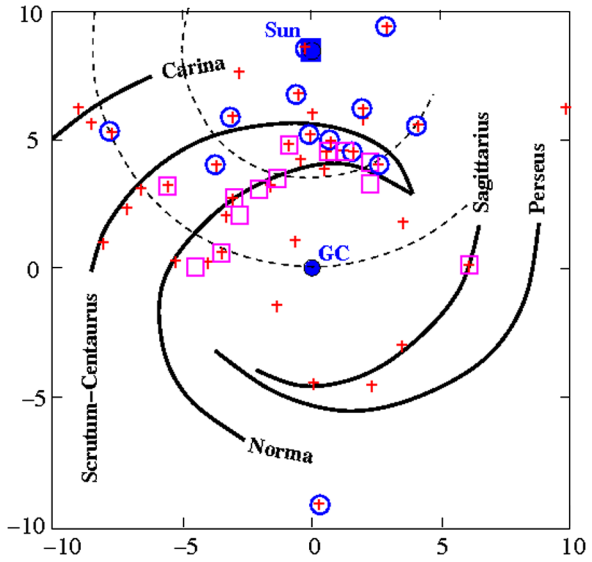

FIG. 14 (color online). Locations of the pulsars associated to the extended sources at 100 GeV on the Galaxy map. Boxes mark the brighter excesses identified in the Fermi data, blue circles correspond to pulsars within weaker VHE γ-ray sources detected by the ground-based γ-ray telescopes. Red crosses mark the positions of known pulsars with ages in the range $T_s < 3 \times 10^4$ yr. The blue circle marks the position of the Galactic center. The blue box is the position of the Sun. Solid curves show the locations of the main arms of the Galaxy. Dashed arcs show the distances 5 kpc and 8 kpc.

TABLE III. List of $T_s < 30$ kyr pulsars positionally coincident with known VHE γ-ray sources

	Name	PSR	R_s	T_s
1	Vela X	B0833 − 45	0.29	1.1
2	G292.2 − 0.5	J1119 − 6127	8.40	0.2
3	HESS J1303 − 631	J1301 − 6305	15.84	1.1
4	HESS J1356 − 645	J1357 − 6429,	4.09	0.7
5	Rabbit	J1418 − 6058		1.0
6	MSH 15 − 52	B1509 − 58	5.8	0.2
7	HESS J1708 − 443	B1706 − 44	1.82	1.8
8	HESS J1741 − 302	B1737 − 30	3.28,	2.1
9	G0.9 + 0.1	J1747 − 2809	≥ 8	0.5
10	HESS J1809 − 193	J1809 − 1943	3.57	1.1
		J1811 − 1925		2.3
11	HESS J1813 − 178	J1813 − 1749		0.5
12	HESS J1833 − 105	J1833 − 1034	4.30	0.5
13	HESS J1846 − 029	J1846 − 0258	5.10	0.1
14	MGRO J1908 + 06	J1907 + 0602	3.01	2.0
15	G54.1 + 0.3	J1930 + 1852	5.00	0.3
16	MGRO J2019 + 37	J2021 + 3651	18.9	1.7
17	Boomerang	J2229 + 6114	3.0	1.1

From Fig. 14 one can see that most of the known nearby supernovae associated with pulsars of the age $T_s \leq 30$ kyr are spatially coincident with excess VHE γ-ray emission. In the case of sources listed in Table II, the emission is extended, with the typical source size in the degree range. This implies the spatial extent $\sim$100 pc at the source distance. Table III includes both isolated (more compact) sources associated to the young pulsar wind nebulae (like e.g. MSH 15 − 52) and extended emission regions discussed above. Further investigation of the nature of emission from these sources is needed.

VII. DISCUSSION

Existence of the 100 pc size extended VHE γ-ray emission regions around the locations of recent injections of TeV CRs in the Galaxy is an immediate testable prediction of the scenario of injection of CRs by the supernovae. These extended emission regions should be visible as degree-scale VHE γ-ray sources with fluxes at the level

of 10^{-11} erg/cm^2 s above 100 GeV. In this paper we have searched for such degree-scale sources in the LAT data. We have found 18 such sources. Table II gives the list of the extended sources found using the MST method. The overall extended source statistics, as well as the morphological properties of sources listed in Table II agree with the theoretical expectations. Based on this agreement, we suggest that the bright extended sources are associated to the sites of recent CR injections in the Galaxy.

The largest part (80%) of the extended VHE γ-ray sources in the Galactic plane, listed in Table II could be associated to pulsars. For 11 out of 15 pulsar-related sources (i.e. 70%) no shell-like SNR structure has been found, which might signify that the supernovae did not result in production of a regular expanding shell (similarly e.g. to the supernova which produced the Crab pulsar). Thus, it is not clear if the presence of a regular shell is an essential ingredient of the CR acceleration process. At the same time, all the shell-type SNRs entering Table II are composite SNRs confining a PWN. None of the sources are associated to shell-like SNR without a pulsar. This might indicate that CR acceleration phenomenon is related to the presence of a pulsar in the SNR.

A significant fraction of pulsars is born in OB associations [50,51]. Young pulsars which have typical birth kick velocities $\leq 10^3$ km/s $=$ 1 pc/kyr do not leave their parent association of the size $\sim$10–100 pc until they reach the age 10^4–10^5 yr. Taking this into account, it is possible that locations of the young pulsar in the Galactic plane just trace the OB associations where they were born. In this case the degree-scale extended γ-ray emission might, in fact, be related to the presence of an OB association or a superbubble, which contains multiple supernova remnants and bubbles blown by the winds of massive stars. The most clear example of this type is given by the extended source in the Cygnus region (source number 8 in Table II). A study of the extended emission in the GeV band, reported bt Ref. [11], finds that cosmic rays were recently injected in this region and suggests that the injection mechanism is related to the multiple shocks produced by the collective effect of winds from massive star filling the Cygnus region superbubble. An alternative possibility, also discussed in the Ref. [11], is that the cosmic rays are produced by the nearby γCygni supernova which hosts PSR J2021 + 4026 (see Sec. V E).

Spatial coincidence of the extended VHE γ-ray sources in the Galactic plane with the pulsars introduces a potential possibility that the extended emission is produced by electrons escaping from the PWN around the pulsar, rather than by CRs filling the 100 pc scale bubble. This possibility requires further investigation. The VHE γ-ray emission in the $E \sim$ 100–300 GeV range could be produced via inverse Compton scattering by electrons of comparable energies upscattering optical-infrared Galactic photon background (photons with energies $\sim$0.1–1 eV). The inverse Compton cooling time of electrons is $\sim 2 \times 10^6$ yr, assuming the density of the optical-infrared background $U \sim 1$ eV/cm^3, typical for the Norma Arm [52]. This cooling time scale is 1 order of magnitude shorter than the CR cooling time (3), calculated assuming the ISM density $n \sim 1$ cm^{-3}. This implies that electrons lose energy more efficiently than protons. To compare the luminosities generated by electrons to those produced by CRs, one needs to know the CR and electron densities in the relevant energy scales, which is highly uncertain. A first guess could be found from the ratio of electron and CR fluxes observed at the Earth: the electron flux at 300 GeV is $\sim 10^{-2}$ of the TeV CR flux [53,54]. Assuming this ratio, one finds that the CR contribution to the extended VHE source flux should dominate over the electron contribution. It is, however, not clear if the locally observed electron-to-nuclei ratio could serve as a good estimate of the ratio close to the distant CR sources. Electrons should still give a dominant contribution to emission from the central parts of the degree-scale sources, at the locations of Crab-like PWNe around the pulsars. Two complementary measurements could be used to separate electron and CR contribution to the VHE γ-ray flux from the degree-scale sources.

First, electron-dominated emission from the central PWN could be identified via radio-to-x-ray observations which could establish the morphology of the PWN and measure the spectrum of the synchrotron emission from high-energy electrons. At larger, degree scales, electrons with energies $E_e \sim 300$ GeV are expected to produce synchrotron emission in the $\epsilon_s \sim 10^{-2}[B/3\ \mu\text{G}] \times [E_e/300\ \text{GeV}]^2$ eV energy range, i.e. in the far infrared (assuming magnetic field $B \sim 3\ \mu$G, typical for the ISM). Detection of the infrared counterparts of the extended VHE γ-ray sources will constrain the electron contribution to the degree-scale VHE source flux.

Alternatively, proton/nuclei contribution to the extended source flux could be measured via detection of neutrino signal from the sources listed in Table II with km^3 scale neutrino detectors like IceCube [55] and km3net [56]. Asuming that most of the γ-ray emission from sources listed in Table II is produced by CR protons/nuclei, the neutrino flux is expected to be comparable to the γ-ray flux given in the column 8 of the Table. This would make the sources from Table II the strongest Galactic neutrino sources. The slope of the neutrino spectrum could be inferred from the HESS observations [26]. The neutrino spectrum produced in nuclei-nuclei interactions is expected to follow the γ-ray spectrum, i.e. to have the power law shape $dN_\nu/dE \sim E^{-2.4}$ in the energy range up to at least ten(s) of TeV. This slope is harder than the slope of the atmospheric neutrino spectrum, so that the sources should be preferably detectable at the highest energies. However, one should note that the source size is expected to increase with energy (see Eq. (5)) making the sources extended for IceCube and km3net.

IceCube is mostly sensitive to the sources in the northern hemisphere. Only two of the 18 sources in Table II are situated in the northern hemisphere: source 8 in the Cygnus region and source 9 associated to HESS J1857 + 026. Currently existing upper limits on the point source fluxes with IceCube 40-string configuration [57] at positions of these sources are still above the expected neutrino flux level, expected to be around $\sim 10^{-11}$ erg/cm^2 s at the energy of 0.1 TeV, and still lower at the energies above 10 TeV at which IceCube is most sensitive.

Possible association of the degree-scale VHE γ-ray sources to pulsar/PWN systems, rather than to the shell-like SNRs without pulsars suggests a possibility that the presence of pulsar plays a significant role in the CR production. PWNe formed by the collisions of pulsar winds with the SNR material and/or with the interstellar medium are known to be very efficient particle accelerators. In these systems most of the energy initially stored as the rotation energy of the neutron star is transferred to the high-energy particles. Most of our knowledge of particle acceleration mechanisms in PWNe is derived from the observations of radio-to-γ-ray emission from the accelerated electrons. In general, the standing relativistic shock at the interface of the pulsar wind and the supernova/interstellar medium should also accelerate protons and heavier nuclei. The energy stored in the rotation of the neutron star is

$$E_{\rm NS} = \frac{I\Omega_{\rm ini}^2}{2} \simeq 3 \times 10^{50} \left[\frac{P_{\rm ini}}{10\ {\rm ms}}\right]^{-2} {\rm erg} \qquad (8)$$

for a typical neutron star with the moment of inertia $I \simeq 1.5 \times 10^{45}$ g cm^2 and the angular velocity $\Omega_{\rm ini} = 2\pi/P_{\rm ini}$ corresponding to the initial rotation period $P_{\rm ini}$. If typical initial periods of the pulsars at birth are in the range $P_{\rm ini} \lesssim 10$ ms, the rotation energy of the neutron star is sufficient for powering the CR production.

Relativistic nature of the shock accelerating CRs could leave an imprint on the CR spectrum in the form of a hardening below the energy corresponding to the gamma factor of the shock [58]. Such a hardening might be responsible for the low-energy break observed in the spectrum of Galactic CRs [5].

Periods of known pulsars increase with time as a power law $P \sim t^{1/(n-1)}$ where n is the breaking index which, for most of the pulsars is in the range $2 \lesssim n \lesssim 3$ [59]. Observations of the power law spin down do not provide information on the initial rotation period of the neutron star at birth. The initial periods of rotation of neutron stars have to be estimated based on numerical modeling of stellar evolution, supernova explosions, and of the subsequent evolution of the neutron stars. Numerical calculations of evolution of massive stars up to the point of gravitational collapse only now start to be able to account for the effects of the stellar rotation. The state-of-art simulations predict the initial period in the range of $P_{\rm ini} \sim 10$ ms for a typical star of 15 solar masses, if a special mechanism for the removal of the angular momentum from the stellar core by strong magnetic field is assumed [48]. Otherwise, the calculations suggest the initial periods in the range of $P_{\rm ini} \sim 1$ ms in the absence of strong magnetic coupling of the core to the outer layers [60].

This implies that the rotation energy of the neutron star could, in principle, provide the power sufficient for production of CRs. If this case the presence or absence of a well-defined SNR shell is not of crucial importance for the acceleration. If the shell is present, the high-energy particles accelerated in the PWN would be confined by the magnetic fields in the shell, where they could interact, like it happens in the MSH 15 − 52/PSR B1509 − 58 system. Otherwise, if the regular shell is not formed (like in the Crab nebula), particles would escape from the PWN directly into the interstellar medium. Alternatively, pulsars might play an ''auxiliary'' role in the CR acceleration process providing an initial injection of ''preaccelerated'' particles in the SNR shell. Understanding of the role of pulsars in the CR acceleration process requires further investigation.

Analysis of abundances of elements in the cosmic ray flux suggests that the bulk of Galactic cosmic rays with energies below 10 GeV is accelerated in the environments containing a mix of supernova ejecta and older interstellar material typically present in OB associations and superbubbles [13,14]. Moreover, the time scale of acceleration is most probably longer than 100 kyr, an observation based on the observation of abundances of specific elements [15]. This implies that low-energy cosmic rays are not produced out of the single supernova ejecta soon after the supernova explosion, but rather originate from the slow acceleration on the system of multiple shocks present in OB associations and superbubbles. Recent Fermi observations of γ-ray emission from the interactions of freshly accelerated cosmic rays in the Cygnus superbubble further support this scenario.

At the same time, recent observations of several breaks in the interstellar cosmic ray spectrum: softening above $\sim$10 GeV [5] and hardening above 200 GeV [54] indicate the presence of multiple components in the cosmic ray spectrum. The component which dominates the low-energy cosmic ray flux and peaks in the 1–10 GeV range has soft spectrum above 10 GeV and becomes subdominant above 200 GeV. It is not clear if conclusion about possible OB associations and/or superbubble origin of the dominant low-energy component holds also at the energies above 200 GeV, or a different acceleration mechanism is relevant at higher energies. As it is mentioned above, association of the degree-scale extended sources with young pulsar might reflect possible OB association membership to the pulsar parent stars, so that multiple acceleration mechanisms related to the pulsar wind nebulae, supernova remnants

and to the entire star-forming region around the supernova/pulsar might be responsible for the production of cosmic rays filling the 100 pc-size regions visible as the degree-scale γ-ray sources.

VIII. CONCLUSIONS

We have considered a possibility of localization of the sources of TeV CRs via detection of degree-scale extended VHE γ-ray emission produced by CRs escaping into the ISM. We have identified extended sources of $E > 100$ GeV γ-rays in the Galactic plane using the data of LAT and studied their statistics and morphological properties. The list of the degree-scale extended source is given in Table II. The average surface brightness profile of the extended sources is shown in Fig. 1.

The observed extended source properties suggest their interpretation as extended emission produced by CRs escaping from relatively young sources of TeV CRs. Most of the degree-scale extended sources are associated to nearby pulsars with the spin-down age $T \lesssim 30$ kyr, as expected in the model of supernova origin of the TeV CRs (if pulsars are considered as tracers of the recent supernova events) *and their star-forming regions*. We find that nearly all known young nearby pulsars are associated to excess extended VHE γ-ray emission. At the same time, none of the detected degree-scale VHE sources is associated to a SNR without a pulsar.

The observed degree-scale extended emission could be produced by both the proton/nuclear CRs and electrons/positrons escaping from the sources. It is difficult to distinguish between the two contributions based on the γ-ray data only. We suggest that the two contributions could be distinguished based on the complementary observations in the infrared band and in the VHE neutrino channel.

ACKNOWLEDGMENTS

We would like to thank F. Aharonian, T. Courvoisier, M. Kachelriess, and A. Taylor for fruitful discussions of the subject and useful comments on the manuscript text. The work of A. N. is supported by the Swiss National Science Foundation Grant PP00P2_123426/1.

[1] V. L. Ginzburg and S. Syrovatskii, *The Origin of Cosmic Rays* (MacMillan, New York, 1964).
[2] V. S. Berezinskii, *Astrophysics of Cosmic Rays* (Eslevier, Amsterdam, 1990).
[3] A. W. Strong, T. A. PorterG. Jóhannesson, P. Martin, I. V. Moskalenko, E. J. Murphy, and E. Orlando, Astrophys. J. **722**, L58 (2010).
[4] P. Blasi and E. Amato, J. High Energy Phys. 01 (2012) 010.
[5] A. Neronov, D. V. Semikoz, and A. M. Taylor, Phys. Rev. Lett. **108**, 051105 (2012).
[6] W. Baade and F. Zwicky, Phys. Rev. **46**, 76 (1934).
[7] F. Aharonian, J. Buckley, T. Kifune, and G. Sinnis, Rep. Prog. Phys. **71**, 096901 (2008).
[8] P. F. Michelson, W. B. Atwood, and S. Ritz, Rep. Prog. Phys. **73**, 074901 (2010).
[9] A. M. Bykov and I. N. Toptygin, Astron. Lett. **27**, 625 (2001).
[10] E. Parizot, A. Marcowith, E. van der Swaluw, A. M. Bykov, and V. Tatischeff, Astron. Astrophys. **424**, 747 (2004).
[11] M. Ackermann *et al.*, Science **334**, 1103 (2011).
[12] Y. Butt, Nature (London) **460**, 701 (2009).
[13] R. E. Linegenfelter and J. C. Hindon, Astrophys. J. **660**, 330 (2007).
[14] W. R. Binns, M E. Wiedenbeck, M. Arnould, A. C. Cummings, G. A. de Nolfo, S. Goriely, M. H. Israel, R. A. Leske, R. A. Mewaldt, E. C. Stone, and T. T. von Rosenvinge, New Astron. Rev. **52**, 427 (2008).
[15] M. E. Wiedebeck W. R. Binns, E. R. Christian, A. C. Cummings, B. L. Dougherty, P. L. Hink, J. Klarmann, R. A. Leske, M. Linjowski, R. A. Mewaldt, E. C. Stone, M. R. Thayer, T. T. von Rosenvinge, and N. E. Yanasak, Astrophys. J. **523**, L61 (1999).
[16] F. A. Aharonian, *Very High Energy Cosmic Gamma Radiation* (World Scientific, Singapore, 2004).
[17] W. B. Atwood *et al.*, Astrophys. J. **697**, 1071 (2009).
[18] V. I. Korchagin *et al.*, Astrophys. J. **126**, 2896 (2003).
[19] K. Nakamura *et al.* (Particle Data Group), J. Phys. G **37**, 075021 (2010).
[20] A. A. Abdo *et al.*, Phys. Rev. Lett. **103**, 251101 (2009).
[21] R. Canipana, E. Massaro, D. Gasparrini, S. Cutini, and A. Trainacere, Mon. Not. R. Astron. Soc. **383**, 1166 (2007).
[22] E. Massaro, F. Tinebra, R. Campana, and G. Tosti, in *Proceedings of the 2009 Fermi Symposium*, econf C091122 (2009).
[23] A. Neronov and D. V. Semikoz, arXiv:1011.0210.
[24] Abdo *et al.* (The Fermi-LAT Collaboration), arXiv:1108.1435 [Astrophys. J. Suppl. Ser. (to be published)].
[25] A. Neronov, D. V. Semikoz, and Vovk Ie., Astron. Astrophys. **529**, A59 (2011).
[26] F. Aharonian *et al.*, Astrophys. J. **636**, 777 (2006).
[27] J. P. Finley and H. Ogelman, Astrophys. J. **434**, L25 (1994).
[28] O. Kargaltsev, G. G. Pavlov, and G. P. Garmire, Astrophys. J. **660**, 1413 (2007).
[29] G. B. Hobbs and R. N. Manchester, ATNF Pulsar Catalogue, http://www.atnf.csiro.au/people/pulsar/psrcat/.
[30] A. A. Abdo, K. S. Wood, M. E. DeCesar, F. Gargano, F. Giordano, P. S. Ray, D. Parent, A. K. Harding, M. Coleman Miller, D. L. Wood, and M. T. Wolf, Astrophys. J. **744**, 146 (2012).

[31] M.-H. Grondin *et al.*, Astrophys. J. **738**, 42 (2011).
[32] F. A. Aharonian *et al.*, Astron. Astrophys. **460**, 365 (2006).
[33] C. L. Brogan, J. D. Gelfand, B. M. Gaensler, N. E. Kassim, and T. J. W. Lazio, Astrophys. J. **639**, L25 (2006).
[34] H. Uchiyama *et al.*, Publ. Astron. Soc. Jpn. **61**, S189 (2009).
[35] E. V. Gotthelf and J. P. Halpern, Astrophys. J. **681**, 515 (2008).
[36] O. Kargaltsev, B. M. Schmitt, G. G. Pavlov, and Z. Misanovic, Astrophys. J. **745**, 99 (2012).
[37] Z. Misanovic, O. Kargaltsev, and G. G. Pavlov, Astrophys. J. **735**, 33 (2011).
[38] R. Mukherjee, E. V. Gotthelf, and J. P. Halpern, Astrophys. J. **691**, 1707 (2009).
[39] W. W. Tian, Z. Li, D. A. Leahy, and Q. D. Wang, Astrophys. J. **657**, L25 (2007).
[40] S. Klepser, J. Krause, and M. Doro, arXiv:1109.6448.
[41] J. W. T. Hessels *et al.*, Astrophys. J. **682**, L41 (2008).
[42] D. A. Green, Bulletin of the Astronomical Society of India **37**, 45 (2009).
[43] Landecker *et al.*, Astron. Astrophys. Suppl. Ser. **39**, 133 (1980).
[44] A. Abramowski *et al.*, Astron. Astrophys. **525**, A46 (2010).
[45] R. Landi, A. De Rosa, A. J. Dean, L. Bassani, P. Ubertini, and A. J. Bird, Mon. Not. R. Astron. Soc. **380**, 926 (2007).
[46] M. Balbo, P. Saouter, R. Walter, L. Pavan, A. Tramacere, M. Pohl, and J.-A. Zurita-Heras, Astron. Astrophys. **520**, A111 (2010).
[47] A. Heger, C. L. Fryer, S. E. Woosley, N. Langer, and D. H. Hartmann, Astrophys. J. **591**, 288 (2003).
[48] A. Heger, S. E. Woosley, and H. C. Spruit, Astrophys. J. **626**, 350 (2005).
[49] L. Bronfman, Astrophys. Space Sci. **313**, 81 (2007).
[50] P. R. Amnuel, O. H. Guseinov, and Iu. S. Kustamov, Astrophys. Space Sci. **121**, 1 (1986).
[51] P. Kaaret and J. Cottam, Astrophys. J. **462**, L35 (1996).
[52] T. A. Porter, I. V. Moskalenko, A. W. Strong, E. Orlando, and L. Bouchet, Astrophys. J. **682**, 400 (2008).
[53] M. Ackermann *et al.*, Phys. Rev. D **82**, 092004 (2010).
[54] O. Adriani *et al.*, Science **332**, 69 (2011).
[55] F. Halzen and S. R. Klein, Rev. Sci. Instrum. **81**, 081101 (2010).
[56] km3Net Technical Design Report, http://www.km3net.org/TDR/TDRKM3NeT.pdf.
[57] R. Abbasi *et al.*, Astrophys. J. **738**, 18 (2010).
[58] M. Lemoine and G. Pelletier, Astrophys. J. **589**, L73 (2003).
[59] A. G. Lyne and F. Graham-Smith, *Pulsar Astronomy*, Cambridge Astrophysics Series (Cambridge University Press, Cambridge, 1998).
[60] G. Meynet (private communication).